Olivine—The Little Green Science Machine

Benoît Welsch[1], Emily C. First[1], Philipp Ruprecht[2], and Michael C. Jollands[3]

Pristine mesostasis-free, plurimillimetric, Fo_{85-87} olivine macrocrysts from Piton Caille, a ~5-ky basaltic vent at Piton de la Fournaise Volcano, Réunion Island. PHOTO: BENOÎT WELSCH.

1811-5209/23/0019-0138$2.50 DOI: 10.2138/gselements.19.3.138

In some ways, olivine has driven the evolution of the Solar System and likely beyond. As one of the earliest-crystallizing silicate minerals, olivine controls the initial chemical evolution of planet-wide magma oceans and individual lava flows alike. In solid aggregate form, it controls and records deformation of the mantle and smaller-scale intrusive complexes. The components of its crystal structure are mobile at high temperatures and their migration can be used to explore the timing of magmatic events. During chemical weathering, these olivine crystals capture carbon dioxide from the atmosphere as secondary minerals are formed. All of these processes take place not only on Earth, but also on other planetary bodies, making olivine ideally suited to shed light on both primordial planet-building processes and current-day volcanism and surface processes.

KEYWORDS: olivine; peridot; mantle; volcano; meteorite; magma differentiation; melt inclusion

INTRODUCTION

Creeping in the mantle, melting into a magma, re-crystallizing in a shallow chamber, erupting from a volcano, breaking down in the subsurface, or orbiting in space: olivine is everywhere and sees everything. As such, it has sparked curiosity and fascination throughout human history. In ancient times, olivine seems to have been one of Cleopatra VII's favorite gemstones, and according to Pliny the Elder, was called "topaz" by the Greeks and Romans when gem-quality crystals were first mined on Zabargad Island (FIG. 1; Revheim 2015). Olivine is even mentioned in the Bible, as "chrysolite," the seventh precious stone adorning the walls of Jerusalem (Revelations 21:20). This name persisted, joined much later by "peridot," an appellation that is still used today by gemologists and jewelers. It was only in the 18th century that the term "olivine" was coined by geologist A.G. Werner, after its common olive-green color. All three names—chrysolite, peridot, and olivine—were finally recognized as the same mineral species thanks to the works of R.J. Haüy and followers on crystal structure. Today, the mineral is still prized as a gemstone and is mined in locations as varied as Myanmar, Pakistan, Norway, Vietnam, and the USA, among others. The highest-quality terrestrial crystals are priced at 50–450 US dollars per carat and up to thousands of US dollars per carat for certified extraterrestrial gemstones. Green olivine of structural formula is both widely available (FIG. 2) and possesses desirable physical, mechanical, and thermal properties. As such, olivine-type materials are used in many innovative technologies and applications, including as an industrial acid waste neutralizer, a cement clinker (known as "belite"), a slag conditioner, a refractory brick (or a raw material for their manufacture, with many patents filed by V.M. Goldschmidt in the 1920s and 1930s), a casting sand, a tap hole filler, a coating material, and as a crystal structure of high power density (the so-called lithium iron phosphate batteries). Beyond these many virtues, the potential of olivine intrigues and it has received ever-increasing attention over the years as a focal point for studying planetary processes, tectonic motions, and magma dynamics—making it arguably the most-studied mineral in Earth sciences. Looking through the olivine lens, this issue of *Elements* presents an array of captivating research.

A ROCK STAR

Olivine is a fundamental building block in the universe: it is found in a wide range of terrestrial rocks, lunar samples, and meteorites (FIG. 2), and has been detected on Mercury, Venus, Mars, and asteroids as well as in debris disks outside of our own Solar System (Demouchy 2021; First et al. 2023 this issue). As planetesimals accrete to form larger bodies, the kinetic energy of their collisions instigates melt formation and even magma oceans. From there, making olivine is a simple recipe. The mineral is relatively frugal and only needs three to four ingredients from the melt: oxygen, silicon, magnesium, and/or iron—a not-so-difficult task given that those four elements are among the ten most abundant in the universe and make up over 90% of Earth's total mass! Thanks to its highly refractory nature and large temperature and pressure stability field (FIG. 3; Bowen and Schairer 1935; Ringwood and Major 1970), olivine would be one of the first minerals to crystallize during subsequent cooling of MgO- and/or FeO-rich silicate melts (e.g.,

1 Macalester College
Geology Department
1600 Grand Avenue
Saint Paul, MN 55105, USA
E-mail: bwelsch@macalester.edu
E-mail: efirst@macalester.edu

2 University of Nevada
Department of Geological Sciences and Engineering
1664 N. Virginia Street
Reno, NV 89557, USA
E-mail: pruprecht@unr.edu

3 Gemological Institute of America
50 W. 47th St
New York, NY 10036, USA
E-mail: mjolland@gia.edu

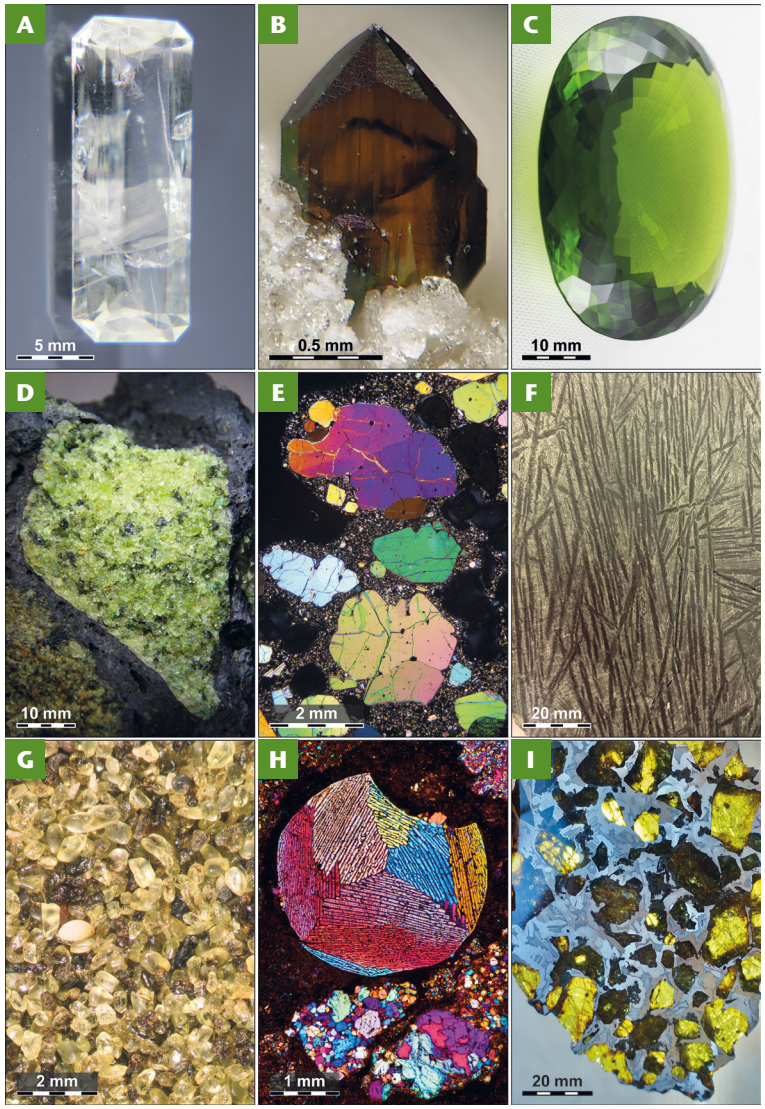

Figure 1 Olivine from across the globe and beyond. (**A**) Gem cut in a colorless forsterite crystal from Mogok, Myanmar. S : J M . (**B**) Clear brown crystal of fayalite from Caspar quarry, Ettringen, Germany. S : W S ; : S W . (**C**) Gem G3398 cut in an olive-green, hydrothermal crystal at $Fo_{90–92}$ from Zabargad Island (Clocchiatti et al. 1981). This is the largest cut reported in the world, with a weight of 311.8 carats (62.35 g). S : S I , NMNH, R F ; P : K L . (**D**) Mantle xenolith from San Carlos Apache Reservation (AZ, USA) made of anhedral olivine grains at $Fo_{87–92}$ and enclosed in a hawaiitic matrix. S : K D ; P : B W . (**E**) Olivine-rich basalt ("oceanite" as de ned by A.F.A Lacroix) from the April 2007 Piton de la Fournaise eruption (Reunion Island) containing large amounts of $Fo_{83–85}$ olivine macrocrysts (Welsch et al. 2013); crossed polar microphotograph of a 30- m thin section. S : OVPF/LGSR; P : B W . (**F**) Long dark blades outlining plate spinifex (A3), Fo_{89} olivine now ghosted by serpentine in Alexo komatiite, Ontario (2.7 Ga). S : F F . (**G**) Sand made of olivine (green), basalt (black), shell and coral (white, brown) fragments from Green Sand Beach (Big Island, Hawaii, USA). S : B W . (**H**) Barred olivine (BO) chondrule in meteorite NWA 2180 (carbonaceous chondrite type CV3) with a composition in the range of $Fo_{91–99}$ (crossed polar microphotograph of a 30- m thin section with a lambda plate). S : M S P P P – P , I ; : B C . (**I**) Polished, etched section of "Tibet" pallasite Gyarub Zangbo containing $Fo_{77–78}$ olivine crystals set in an iron–nickel matrix (kamacite and taenite displaying a Widmanstätten pattern). S : S J .

Elkins-Tanton et al. 2003) and thus initiate magmatic di erentiation as described by N.L. Bowen's reaction series.

The virtual ubiquity of olivine (F . 2) makes it prone to experience a large variety of physical and chemical processes, and studies of its fundamental characteristics have helped to unravel many scienti c mysteries. For instance, the parametrization of olivine's physical properties allowed seismologists to identify peridotites (olivine-rich rocks) as the main component of Earth's upper mantle based on the propagation and reconstruction of P- and S-waves, corroborating the abundance of olivine in xenoliths in rapidly ascending magmas (e.g., kimberlites). Olivine-rich rocks are an integral part of Earth's inner workings, as they accommodate mantle motion and continuous sliding of the tectonic plates (see Demouchy et al. 2023 this issue). In the mantle below oceanic ridges, hotspots, and subduction zones, a fraction of these peridotites melt and produce magmas saturated in olivine components. When these magmas ascend and cool on their way to the surface, they reprecipitate olivine again, this time as a building block of plutonic and volcanic rocks in the crust (Ruprecht and Welsch 2023 this issue). The life cycle of olivine, however, ends at the surface when the mineral comes into contact with water over protracted periods of time and gradually loses its structural and chemical integrity (Plümper and Matter 2023 this issue). As it bids farewell, olivine may transform itself into a crucial agent for the emergence of life, along with other key minerals such as bridgmanite, serpentine, and pyrrhotite (e.g., Russell and Ponce 2020). Considering its wide-ranging origins and applications, olivine is at the intersection of many elds of research and interests. Much as *Drosophila* (the fruit y) has been instrumental to the biological sciences, so too has olivine become a primary reference in many geological elds: defects and di usion (Chakraborty 2008), planetary science, spectroscopy, rock mechanics, crystal growth and dissolution, melt inclusion studies, volcano petrology, and more. In many regards, this little green mineral represents an outstanding vessel to reach and explore a variety of environments that would be otherwise inaccessible to scientists. Before diving deeper into the olivine world with the next chapters, we present below an overview of its main characteristics.

STRUCTURE

The periodic arrangement of atoms making up the Bravais lattice of minerals, determined by X-ray diffraction around 100 years ago, can now be viewed directly using transmission electron microscopy (F . 4). At the atomic scale, minerals of the olivine group are usually built on a framework of tetrahedron-shaped units made of one central silicon cation and four oxygen anions placed at the apices, connected, and brought to neutrality with a pair of divalent cations in two distinct octahedral (i.e., metal, M) sites, denoted M1 and M2 (F . 4; Deer et al. 1982). The olivine structure is that of a nesosilicate (formerly known as "orthosilicate"), in which each silicate tetrahedron is independent ("neso" meaning "island" in Greek) and only

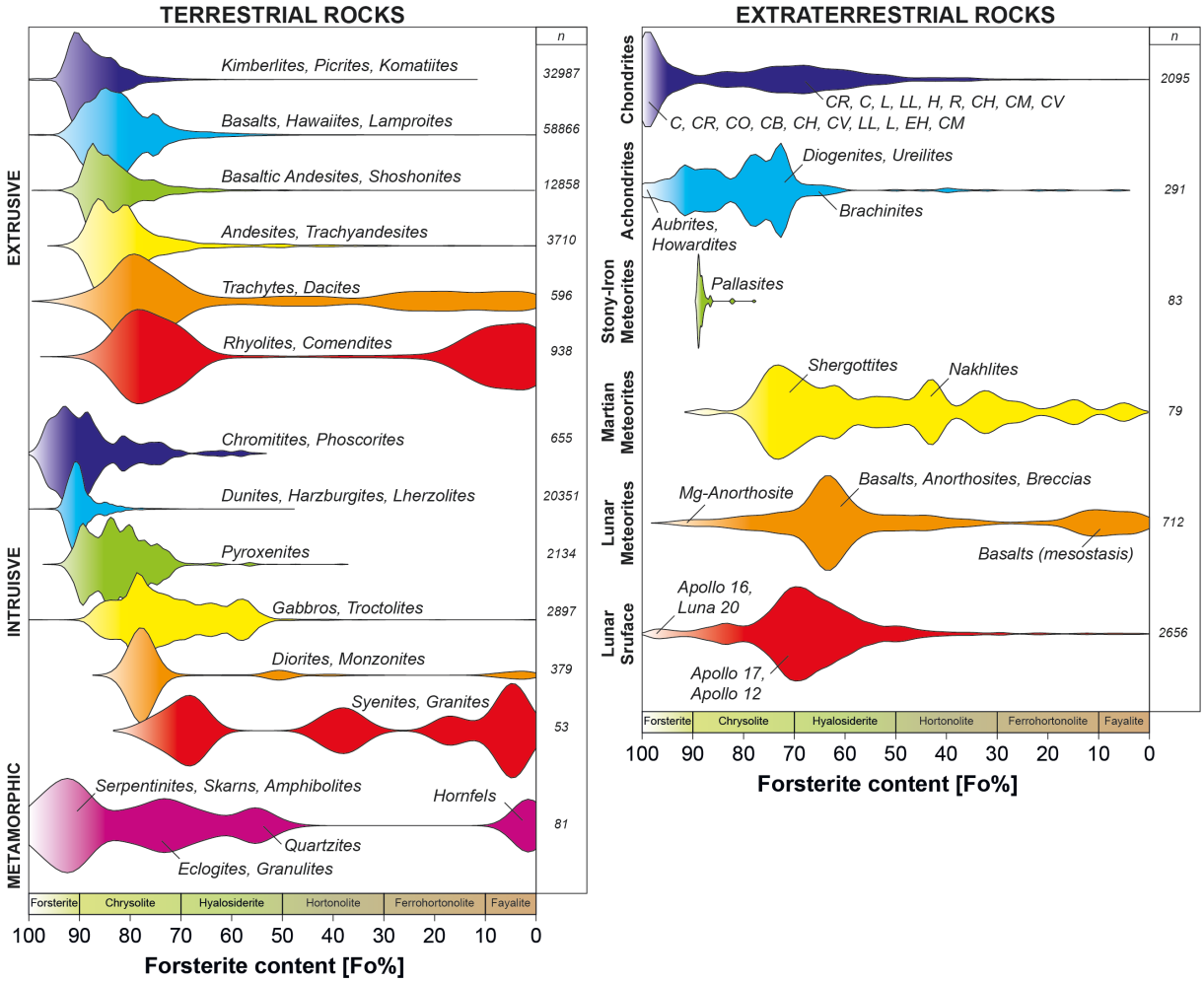

Figure 2 Forsterite content and name types of olivine (Deer et al. 1982) in terrestrial and extraterrestrial rocks based on the GEOROC (DIGIS Team 2021) and Astromat (www.astromat.org) databases, with the three dominant rock types given in order of abundances of analysis (n) within each group of rocks (e.g., $n_{Basalts} > n_{Hawaiites} > n_{Lamproites}$ in the ma c extrusive group). Both datasets were curated using the following criteria: (1) total oxides must comprise between 98 and 101 wt%; (2) sum of main olivine components (SiO_2 + MgO + FeO) must be 90 wt%; (3) total of cations for 4 oxygens must comprise between 2.95 and 3.05. For terrestrial rocks, the chemical analyses (total number n ~ 136k) were subdivided into groups of rocks following the TAS (total alkali versus silica) classi cation. Each rock is often associated with a range of olivine compositions that suggests di erent crystal populations (see Ruprecht and Welsch 2023 this issue), with, for instance, forsteritic olivine in rhyolites interpreted as foreign crystals extracted by silicic magmas during their ascent (e.g., Davì et al. 2010). For extraterrestrial olivine, the data (total number n ~ 6k) was downloaded in January 2023, and the samples were cross-referenced and classi ed into groups using the Meteoritical Bulletin Database (https://www.lpi.usra.edu/meteor/metbull.php). Chondrites include the groups EH, H, L, LL, C, CM, CV, CR, CO, CB, CH, and R. Achondrites includes primitive achondrites (acapulcoites, lodranites, winonaites, ureilites, and brachinites) and asteroidal achondrites (howardites, eucrites, diogenites [HED], angrites, and aubrites). Stony-iron meteorites are pallasites only. Martian meteorites are shergottites, nakhlites, and chassignites (SNC). Samples collected on the Moon surface include those taken by Apollo missions 11, 12, and 14–17, and Luna 16, 20, and 24. Those samples and the lunar meteorites are basalts, anorthosites, gabbros, and breccias. See Jollands et al. (2023 this issue) for a trace element plot.

connected to each other by the metal cations—a major di erence to the other silicate structures, in which the tetrahedrons are bridged to each other by oxygen anions along speci c patterns. In olivine, the smallest portion of the framework that contains the same three-dimensional pattern and that is repeated periodically in the entire crystal is a unit cell of orthorhombic symmetry containing four formula units (Z) of silicate tetrahedrons with their pairs of metal ions (F . 4). The orthorhombic symmetry of olivine means that its structure is di erent when viewed down the three principal axes, described as *a*, *b*, and *c*. As a note of caution, the structural symmetry of olivine can be described with di erent space groups, traditionally *Pbnm* among geologists and *Pnma* among material scientists. This di erence implies that the cell parameters are of the type $a < c < b$ with *Pbnm* and $c < b < a$ with *Pnma*, which can be at the root of unfortunate indexing and miscommunications, as discussed in Yasutake et al. (2019).

CHEMISTRY

At a scale greater than the unit cell, the compound mixture of formula units forms a complete solid solution between the two pure end-members situated in the M1 and M2 sites (F . 4). Olivine crystals of the $[(Mg,Fe)_2SiO_4]$ series are the most common variety in nature, with forsterite as the magnesium end-member ($[Mg_2SiO_4]$, noted Fo_{100}) and fayalite as the iron end-member $[Fe_2SiO_4]$, equivalent to Fo_0). Compound mixtures are graded based on their relative molar fraction in end-member cations (here pure magnesium and pure iron), with the forsterite content (Fo) being traditionally obtained from electron microprobe spot analyses by converting the measured weight percent of the two end-members' oxides (wt.% MgO, wt.% FeO) into cation mole fraction (X_{Mg}, X_{Fe} normalized to four oxygens) and calculating Fo as $Fo = 100 \times X_{Mg}$ $(X_{Mg} + X_{Fe})$. This term can be also referred as the Mg number (Mg#), although it is more commonly used for other ferromagnesian, solid

solution minerals (such as pyroxenes and amphibole), and for bulk rock compositions—serving in a similar way to a differentiation and temperature index. As another note of caution, the classic binary phase diagram gives olivine compositions in weight percent Fo–Fa (FIG. 3), which differ from true Fo content based on molar fraction.

The color intensity of olivine crystals increases with increasing proportion of Fe in its structure, from colorless in pure forsterite to clear brown in pure fayalite, with the intermediate compositions spanning different shades of green (FIG. 1A–1C), and divided in up to six ranges and olivine types (FIGS. 2 and 3). As an umbrella term for each solid solution series of the olivine group, the term "olivine" itself is not listed as a mineral species by the International Mineralogy Association (IMA; Demouchy 2021), rather only its pure end-members. As shown in FIGURE 2, the majority of olivine compositions reported in terrestrial rocks are in the range ~$Fo_{96–70}$, with forsteritic olivine ($Fo_{>50}$) occurring essentially in ultramafic to intermediate rocks and fayalitic olivine ($Fo_{<50}$) only found in felsic rocks. Other cations such as Mn^{2+} (end-member: tephroite [Mn_2SiO_4]) and Ca^{2+} (end-member: larnite [Ca_2SiO_4]) can lead to distinct olivine series with unique associations in the Solar System, such as the CaFe–CaMg series with kirschteinite [$(Ca,Fe)_2SiO_4$] occurring in angrite meteorites and monticellite [$(Ca,Mg)_2SiO_4$] in kimberlites. The whole range of olivine compositions can be found in metamorphic rocks (FIG. 1), a likely result of a wide diversity in protoliths subject to different meta-processes of variable intensity (e.g., hydrothermal alteration of peridotites in Clocchiatti et al. 1981; precipitation from volcanic fluids in rhyolites in Martin et al. 2015; contact metamorphism of dolomites in Beno et al. 2020). By capturing only Fe^{2+}, [$(Mg,Fe)_2SiO_4$] olivine also has the lowest $Fe^{3+}/\Sigma Fe$ ratio of any major ferromagnesian mineral, which concentrates Fe^{3+} in the residual liquid as olivine crystallizes. This drives the melt to higher oxygen fugacity as three O^{2-} are bound by two Fe^{3+}, versus two O^{2-} being bound by two Fe^{2+}, in the liquid. Depending on the presence of other minerals to buffer this higher oxygen fugacity, planetary bodies that form an olivine mantle may hence render to the surface a flow of oxidized volatiles such as H^+ and C^{4+}, with CO_2 being the main substrate for life (e.g., Russell and Ponce 2020). Because olivine often starts draining components from the melt before any other minerals have a chance to form (e.g., pyroxenes, plagioclase), the signal for its crystallization can be one-dimensional and unobscured when looking at bulk rock and glass compositions. Although olivine is highly selective regarding the elements that can enter its structure, it can incorporate small amounts of P, Al, Cr, and H, among other traces (Bell and Rossman 1992; Milman-Barris et al. 2008; Demouchy et al. 2023 this issue; Jollands et al. 2023 this issue). Analysis of these trace elements in the residual melt allows tracking back to sources and magmatic processes (e.g., O'Neill and Jenner 2016; Ruprecht and Welsch 2023 this issue).

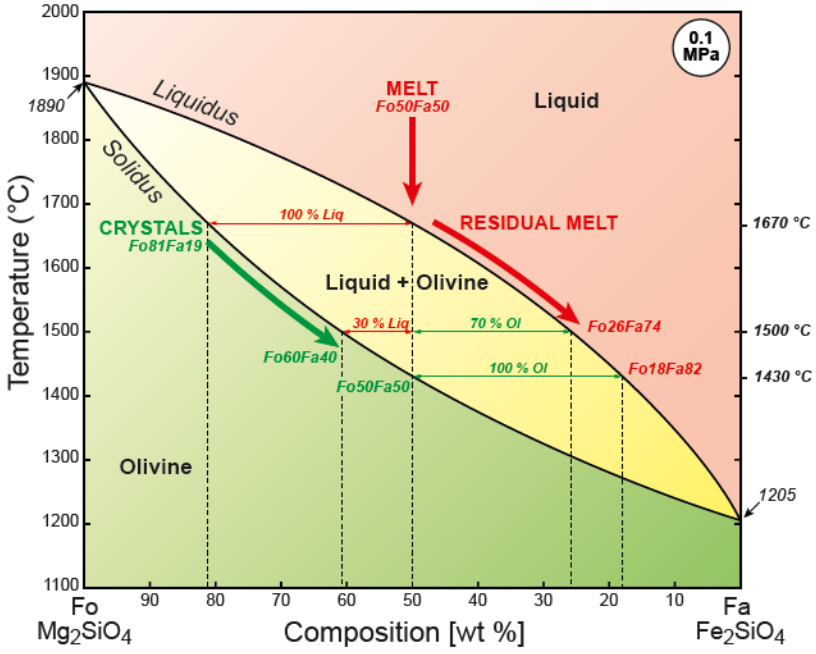

FIGURE 3 Binary phase diagram of Mg_2SiO_4–Fe_2SiO_4 at 0.1 MPa after Bowen and Schairer (1935). Taking an example of the cooling down of a silicate melt of composition Fo50Fa50, crystallization starts at 1670 °C with Fo81Fa19 olivine (note that those are not the true Fo contents). This melt composition, along with that of the solids, evolves along the curves of the liquidus and solidus, respectively, such as at 1500 °C, the solid fraction is at Fo60Fa40 and makes up 70% of the initial mass for a residual melt at Fo26Fa74 and 30% of the mass (using the lever rule). The liquid would reach complete solidification at ~1430 °C.

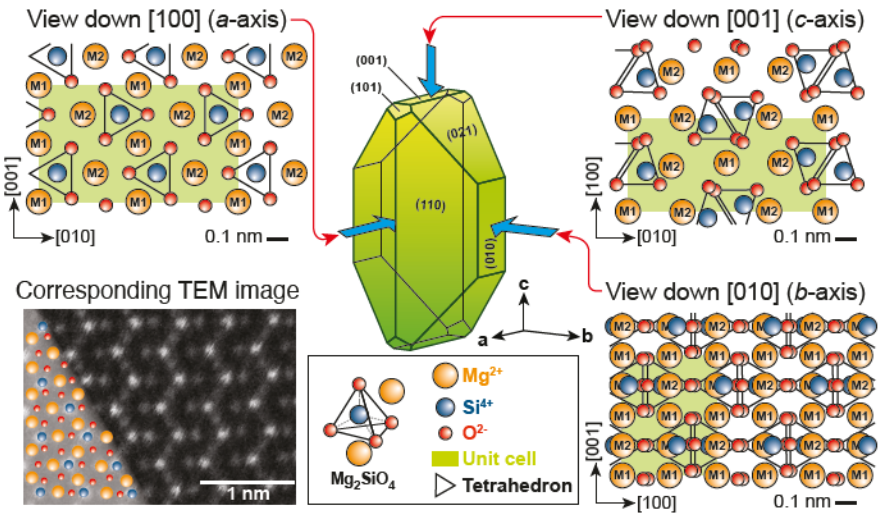

FIGURE 4 Atomic structure of olivine assuming pure forsterite and viewed parallel to the three principal crystallographic axes *a*, *b*, and *c*, in the *Pbnm* space group. The ions O^{2-} have been shrunk and the ions Si^{4+} enlarged for visualization; the real ionic radii are Mg^{2+}: 0.72 Å; Si^{4+}: 0.26 Å; and O^{2-}: 1.38 Å. The ions Mg^{2+} occupy all M1 and M2 sites. The atomic structures are determined by X-ray diffraction, but can also be imaged directly using transmission electron microscopy (TEM), where Si^{4+} appears as bright circles and Mg^{2+} as slightly darker spots (looking down the [100] direction). The 2D-projections of the orthorhombic unit cell appear in green, with Z = 4 the number of formula units within. Atomic structure modeled with VESTA 3 software (Momma and Izumi 2011), with labels following interactive structures on https://www.mindat.org. Scanning transmission electron microscopy (STEM) image collected with the atomic resolution electron microscope (ARM) JEOL JEM-2010F at Jožef Stefan Institute by Goran Dražić and Nina Daneu. Crystal modeled from Welsch et al. (2013). The Miller indices (*hkl*) refer to singular faces and planes, {*hkl*} indicate a set of symmetry-equivalent faces or "forms," [*uvw*] correspond to a singular direction, and <*uvw*> are a set of symmetry-equivalent directions.

CRYSTAL FEATURES

At the micro- to macroscopic scale, an olivine crystal may adopt a wide range of geometrical shapes as a function of its environment of crystallization and storage, from anhedral grains in mantle and crustal peridotites to blades and hybrid growth forms in magmas and lavas (F . 1B, 1D–1F, 1H, 1I; Welsch et al. 2013; Demouchy et al. 2023 this issue; Ruprecht and Welsch 2023 this issue). When crystallizing slowly from a silicate melt, its equilibrium habit is polyhedral and can be made by up to 20 faces (16 in F . 4): four {110}, four {121}, four {120}, two {010}, four {101}, and two {001} (see crystallographic nomenclature in F . 4's caption). Olivine can also experience structural errors early during its crystal growth, which leads to simple twinning laws on re ection planes revolving around the *a*-axis: {021} (formerly identi ed as {100}), {011}, {012}, and {031}; Deer et al. 1982; Welsch et al. 2013). Perhaps one of the most important attributes of olivine is that this mineral is a premium target to probe the chemical composition of parental magmas thanks to its high capability to embay pockets of surrounding material comprising melt, uid, bubbles, and other solids (e.g., spinel, magnetite) and seal them o as inclusions during its crystal growth (e.g., Roedder 1965, 1979). For many decades now, olivine-hosted melt, uid, and solid inclusions have proven to be powerful tools to constrain the petrogenesis of crystals and rocks that contain them, and to access the chemistry of their past environments (e.g., Clocchiatti et al. 1981; First et al. 2023 this issue; Ruprecht and Welsch 2023 this issue).

LIMITS

Olivine is generally hard (6.5–7 on the Mohs scale) and has poor cleavage in the primary planes {100}, {010}, and {001} (Deer et al. 1982). Forsteritic olivine is also prone to alteration upon which its color changes to pale green or red-brown as it is replaced by serpentine (a phyllosilicate formed by hydration, see Plümper and Matter 2023 this issue), or iddingsite (a mixture of clay minerals, iron oxides, and ferrihydrites formed through progressive oxidative weathering; Smith et al. 1987), respectively. Alternatively, alteration may a ect only the iron contained in olivine, forming hematite, magnetite, and sometimes laihunite by oxidation, turning the crystal dark and opaque (e.g., Martin et al. 2015) and leading the remaining parts to become more enriched in MgO proportionally to FeO (e.g., Plechov et al. 2018).

The density of olivine increases with its Fe content, from 3.3 to 4.4 g/cm^3, and its melting point decreases, from 1890 °C in pure forsterite to 1205 °C in pure fayalite in the simple system MgO–FeO–SiO_2 at atmospheric pressure (0.1 MPa, F . 3; Bowen and Schairer 1935). In more complex systems, such as terrestrial magmas, the liquidus of olivine is depressed, with upper bounds on the order of 1620 °C in komatiites, 1300 °C in basalts, and 1000 °C in rhyolites, at 0.1 MPa (Martin et al. 2015; Sossi and O'Neill 2016). Modeling (Bowen and Schairer 1935) and high-pressure experiments (Akimoto et al. 1967; Ringwood and Major 1970) indicate that the liquidus of forsterite and fayalite also increase with pressure, by 41–48 and 35–75 °C/GPa, respectively. The olivine unit cell becomes more compact with the pressure increases, which leads to polymorphic phase transformations (i.e., change in crystal structure for a same stoichiometry). On Earth, olivine (α – [$(Mg,Fe)_2SiO_4$], orthorhombic nesosilicate) is stable from the surface to 410 km depth (14 GPa); from 410 to 520 km (18 GPa), it is replaced by wadsleyite ([β – $(Mg,Fe)_2SiO_4$]), orthorhombic sorosilicate); and from 520 to 670 km (23 GPa), it is transformed into ringwoodite (γ – [$(Mg,Fe)_2SiO_4$], cubic nesosilicate). The $(Mg,Fe)_2SiO_4$ stoichiometry is not stable beyond that depth and is instead dissociated into two separate phases, bridgmanite and magnesiowüstite, with $(Mg,Fe)_2SiO_4 \rightarrow (Mg,Fe)SiO_3 + (Mg,Fe)O$.

OUTLINES

In this issue of *Elements*, we begin our exploration of olivine with a lattice-scale look at trace element incorporation and migration in Chapter 2 (Jollands et al. 2023). This naturally segues into Chapter 3 (Demouchy et al. 2023), which presents crystal defects and deformation in the most primitive and perhaps fundamental olivine on our own planet, that of Earth's upper mantle. Studies of element zoning and di usive timescales are a key component of Chapter 4 (Ruprecht and Welsch 2023), which focuses on magmatic olivine and its ability to preserve information about entire systems from source to surface (P, T, fO_2, composition, etc.) in a way that is useful to volcanologists. After olivine erupts, or is exposed at Earth's surface by uplift and erosion, it is subject to alteration in our atmosphere and hydrosphere; these interactions capture CO_2 and convert it into solid minerals, providing a potential storage point for anthropogenic carbon. The fate of olivine in the subsurface and its role in carbon sequestration represents a big question mark in recent studies, as discussed in Chapter 5 (Plümper and Matter 2023). Finally, in Chapter 6 (First et al. 2023), all of the previous topics are applied beyond Earth to understand early Solar System processes, our own Moon and neighboring planets, and potentially exoplanet surfaces and atmospheres across our Galaxy.

ACKNOWLEDGMENTS

We extend our sincere gratitude to the editors, authors, and content creators, who kindly participated in this issue of *Elements*. We are grateful to Hugh O'Neill and an anonymous reviewer for improving the quality of an earlier version of this manuscript. BW bene ted from NSF awards #1650416 and #1902278. ECF was supported by the Heising-Simons foundation via a 51 Pegasi b Fellowship. PR acknowledges NSF awards #1426820 and #2147714.

REFERENCES

Akimoto S, Komada E, Kushiro I (1967) E ect of pressure on the melting of olivine and spinel polymorph of Fe_2SiO_4. Journal of Geophysical Research 72: 679-686, doi: 10.1029/JZ072i002p00679

Bell DR, Rossman GR (1992) Water in Earth's mantle: the role of nominally anhydrous minerals. Science 255: 1391-1397, doi: 10.1126/science.255.5050.1391

Beno CJ, Bowman JR, Loury PC, Tapanila LM, Fernandez DP (2020) Evidence for dendritic crystallization of forsterite olivine during contact metamorphism of siliceous dolostones, Alta stock aureole, Utah. Contributions to Mineralogy and Petrology 175: 93, doi: 10.1007/s00410-020-01734-9

Bowen NL, Schairer JF (1935) The system MgO-FeO-SiO_2. American Journal of Science s5-29: 151-217, doi: 10.2475/ajs.s5-29.170.151

Chakraborty S (2008) Di usion in solid silicates: a tool to track timescales of processes comes of age. Annual Review of Earth and Planetary Sciences 36: 153-190, doi: 10.1146/annurev.earth.36.031207.124125

Clocchiatti R, Massare D, Jehanno C (1981) Origine hydrothermale des olivines gemmes de l'île de Zabargad (St. Johns) Mer Rouge, par l'étude de leurs inclusions. Bulletin de Minéralogie. 104, 354-360

Deer WA, Howie RA, Zussman J (1982) Rock-forming minerals: orthosilicates. Second Edition. Geological Society of London, 919 pp

Davì M, De Rosa R, Holtz F (2010). Ma c enclaves in the rhyolitic products of Lipari historical eruptions; relationships with the coeval Vulcano magmas (Aeolian Islands, Italy). Bulletin of Volcanology 72: 991-1008, doi: 10.1007/s00445-010-0376-5

Demouchy S (2021) Defects in olivine. European Journal of Mineralogy 33: 249-282, doi: 10.5194/ejm-33-249-2021

Demouchy S, Wang Q, Tommasi A (2023) Deforming the upper mantle: olivine mechanical properties and anisotropy. Elements 19: 151-157

DIGIS Team (2021) 2022-03-SGFTFN_OLIVINES.csv. GEOROC Compilation: Minerals: Göttingen Research Online / Data, doi: 10.25625/SGFTFN

Elkins-Tanton LT, Parmentier EM, Hess PC (2003) Magma ocean fractional crystallization and cumulate overturn in terrestrial planets: implications for Mars. Meteoritics and Planetary Science 38: 1753-1771, doi: 10.1111/j.1945-5100.2003.tb00013.x

First E, Kremer C, Telus M, Trang D (2023) Galaxy of green. Elements 19: 173-179

Jollands MC, Dohmen R, Padrón-Navarta JA (2023) Hide and seek: trace element incorporation and di usion in olivine. Elements 19: 144-150

Martin AM and 5 coauthors (2015) Fayalite oxidation processes in Obsidian Cli s rhyolite ow, Oregon. American Mineralogist 100: 1153-1164, doi: 10.2138/am-2015-5042

Milman-Barris M and 7 coauthors (2008) Zoning of phosphorus in igneous olivine. Contributions to Mineralogy and Petrology 155: 739-765, doi: 10.1007/s00410-007-0268-7

Momma K, Izumi F (2011) VESTA 3 for three-dimensional visualization of crystal, volumetric and morphology data. Journal of Applied Crystallography 44: 1272-1276, doi: 10.1107/S0021889811038970

O'Neill HSC, Jenner FE (2016) Causes of the compositional variability among ocean oor basalts. Journal of Petrology 57: 2163-2194, doi: 10.1093/petrology/egx001

Plechov PY, Shcherbakov VD, Nekrylov NA (2018) Extremely magnesian olivine in igneous rocks. Russian Geology and Geophysics 59: 1702-1717, doi: 10.1016/j.rgg.2018.12.012

Plümper O, Matter JM (2023) Olivine—the alteration rock star. Elements 19: 165-172

Revheim O (2015) Peridot from St. John's / Zabargad Island. https://www.mindat.org/article.php/2053/Peridot+from+St.+John%27s+_+Zabargad+Island. Retrieved February 23, 2023

Ringwood AE, Major A (1970) The system Mg_2SiO_4–Fe_2SiO_4 at high pressures and temperatures. Physics of the Earth and Planetary Interiors 3: 89-108, doi: 10.1016/0031-9201(70)90046-4

Roedder E (1965) Liquid CO_2 inclusions in olivine-bearing nodules and phenocrysts from basalts. American Mineralogist 50: 1746-1782

Roedder E (1979) Origin and signi cance of magmatic inclusions. Bulletin de Minéralogie 102: 487-510

Ruprecht P, Welsch B (2023) Olivine exit interviews—piecing together magmatic puzzles. Elements 19: 158-164

Russell MJ, Ponce A (2020) Six 'must-have' minerals for life's emergence: olivine, pyrrhotite, bridgmanite, serpentine, fougerite and mackinawite. Life 10: 291, doi: 10.3390/life10110291

Smith KL, Milnes AR, Eggleton RA (1987). Weathering of basalt: formation of iddingsite. Clays and Clay Minerals 35: 418-428, doi: 10.1346/CCMN.1987.0350602

Sossi PA, O'Neill HSC (2016) Liquidus temperatures of komatiites and the e ect of cooling rate on element partitioning between olivine and komatiitic melt. Contributions to Mineralogy and Petrology 171: 49, doi: 10.1007/s00410-016-1260-x

Welsch B, Faure F, Famin V, Baronnet A, Bachèlery P (2013) Dendritic crystallization: a single process for all the textures of olivine in basalts? Journal of Petrology 54: 539-574, doi: 10.1093/petrology/egs077

Yasutake M, Miyake A, Mikouchi T, Tsuchiyama A (2019) Notice on the EBSD analysis of olivine in meteorites. 82nd Annual Meeting of The Meteoritical Society. LPI Contribution 2157 ■